

Design Scaling Laws for Self-Phase Modulation-based 2R-Regenerators

Lionel Provost, Christophe Finot, Periklis Petropoulos, David J. Richardson

Optoelectronics Research Centre, University of Southampton, Southampton, SO17 1BJ, United-Kingdom

lap@orc.soton.ac.uk

Abstract We report global scaling laws linking the design of SPM-based 2R-regenerators to their ability to reduce amplitude noise and improve the signal extinction ratio.

Introduction

All-optical 2R-regeneration is anticipated to be an important function within future optical networks. Among the proposed technical solutions, the approach based on Self-Phase Modulation (SPM) and offset filtering in normally dispersive fibres appears particularly attractive because of the ease of implementation for RZ signals [1]. However, despite numerous experimental papers, there have only been a few works which address design issues for such regenerators [2, 3], and there remains a lack of a global design chart that links the regeneration performance to the physical design parameters. In this paper, we report scaling laws for the design of SPM-based regenerators and link these to simple system performance metrics.

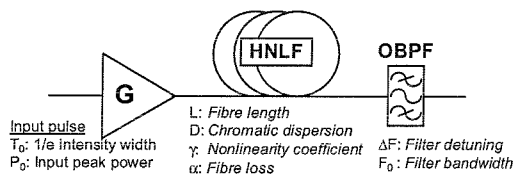


Fig. 1. SPM-based 2R-regenerator stage.

Basic principles

Fig. 1 depicts the idealised SPM-based 2R-regenerator stage considered herein. A stream of data pulses exhibiting amplitude noise, and a specified finite one-to-zero bit extinction ratio, is amplified and fed into a highly-nonlinear fibre (HNLF). Reshaping of the individual data pulses is achieved by filtering the SPM-induced broadened spectrum using a filter detuned by a frequency ΔF relative to their central frequency. Due to the dependence of the spectral broadening on the input pulse peak power, the filter position allows discrimination between one and zero bit levels (thus improving the output extinction ratio), and compression of the amplitude noise on the ones. Noise suppression is favoured if the SPM-broadened pulse spectrum has a flat-top, which dictates the use of HNLF with normal dispersion [4]. The primary customisable regenerator parameters are shown in Fig.1. The input pulse shape should also be added to these, since this will affect the evolution of the spectral broadening. In this work, we have considered transform-limited Gaussian input pulses, however the general trends described should also apply to other pulse forms.

Regenerator parameters

In the following, we present the results of simulations to assess the system performance of a regenerator as a function of its physical characteristics. The general performance of a 2R regenerator can be quantified by means of the power Transfer Function (TF) (output vs. input pulse peak power) of the system. Depending on the various parameter settings, we distinguish three possible forms of TF behaviour depending on the detailed nonlinear pulse evolution and the resulting interplay with the filtering process (see Fig.2): A) non-monotonic variation; B) locally flat; or C) a monotonic variation with input peak power. Generally speaking, a B-type TF will give optimum performance in terms of amplitude noise suppression on the ones. However, apart from this requirement, the optimal regenerator must also be designed to provide i) sufficient extinction for the zeros; and ii) reasonable energy efficiency.

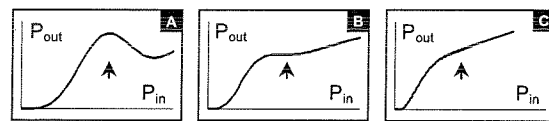


Fig. 2. Possible 2R regenerator power TF types. Associated nominal input peak powers P_1^{in} are marked by the arrows.

In order to parameterise the TF, we first set the nominal input peak power for the one bits P_1^{in} at the point where the absolute value of the derivative of the TF is minimised. We can then define ρ as the relative output power variation for input pulse powers ranging by $\pm 7.5\%$ around P_1^{in} ; and ER^{out} as the output extinction ratio value between one and zero bits when the input extinction ratio $ER^{in}=0.1$. These parameters are shown schematically in Fig. 3.

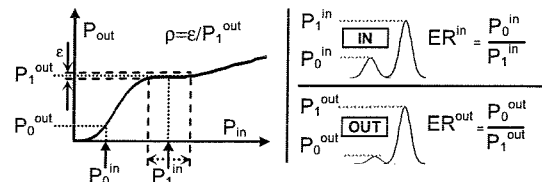


Fig. 3. Considered parameters for power transfer function (left). Associated ER definitions for input and output pulses (right).

We have limited our numerical model of the nonlinear propagation to considering the effects of pure second order group velocity dispersion and SPM. We have

considered the HNLF to be lossless and to have normal group velocity dispersion. The output filter is assumed to have a Gaussian shape, with a $1/e$ -width F_0 equal to that of the input pulses - i.e. $F_0=1/(2\pi T_0)$. Our calculations show that the key TF parameters of the regenerator can be related to its physical properties by the normalised quantities $N=(L_D/L_{NL})^{1/2}$, the ratio L/L_D and the normalised filter position $\Delta F/F_0$ (here $L_D=2\pi c T_0^2/[\lambda^2 D]$, and $L_{NL}=1/\gamma P_1^{in}$ are the dispersive and nonlinear lengths respectively [5]). These relationships are shown in the multidimensional contour plot of Fig.4.

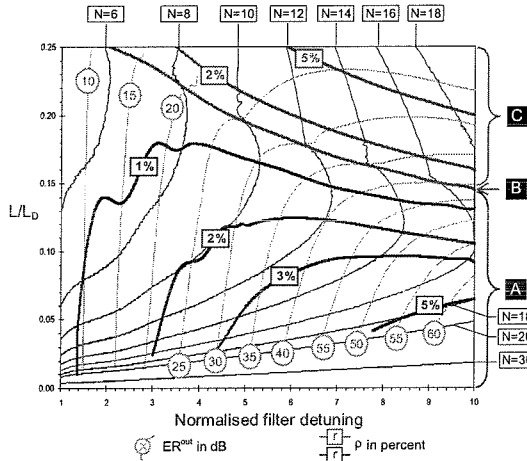


Fig. 4. Multi-contour diagram in L/L_D -Normalised filter detuning ($\Delta F/F_0$) space. Output ER^{out} ratios (in dB) are circled-values. N curves are reported from $N=6$ to $N=30$. Relative TF output peak-to-peak power variations for marks are reported in percents (bold lines) with corresponding TF type zones.

Discussion

Fig. 4 provides clear guidelines linking the physical parameters to the regeneration performance. For example, a type-B TF with a 30dB output ER^{out} is achieved for $L \sim 0.18L_D$ and $\Delta F \sim 6.3F_0$. Under these conditions P_1^{in} should be such that $N \sim 12$.

Following our TF parameterisation, there are a few points worth emphasizing. Firstly, a B-type TF appears to be attainable for various N values. Further, the fibre lengths that satisfy this regime scale as $L_D \cdot (N_0/N)^{1/2}$, where $N_0=0.382$ (with a $\pm 4\%$ error for $N=5.5$ up to $N=23$). The normalised filter detuning exhibits a linear dependence on N , similar to the observation in [3]. Secondly, the sensitivity of ρ (and TF type) to the fibre length is greatest when L_D is large (e.g. long pulses or a small dispersion value). Thirdly, although ER^{out} remains principally determined by the filter position $\Delta F/F_0$, lower ER^{out} is obtained for the same N -value and filter position, when shifting from A to C-type TFs.

Finally, we have studied the scaling of the energy efficiency of the regenerator to its physical parameters. By its nature, the SPM-based 2R regenerator is known to exhibit poor energy efficiency (i.e. output/input energy ratio of the ones), and the

higher the offset ΔF the lower this becomes. It is also clear that a trade-off between ER^{out} and energy efficiency exists. Assuming that the system is operating within the B-type TF regime, then the energy efficiency can be expressed as a function of N , as shown in Fig. 5.

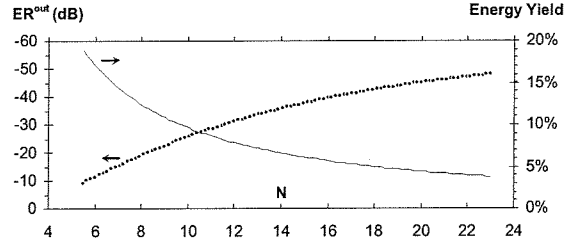


Fig. 5. Extinction ratio and output/input power yield for B-type TF vs. N number.

Our simulations show that the reported scaling law trends are preserved when fibre losses are included. However, as compared to the lossless case, for the same N value in the B-type TF regime, it becomes necessary to increase L/L_D and decrease $\Delta F/F_0$ in order to achieve similar levels of system performance to compensate for SPM spectrum changes. Other aspects of our work have shown that minimisation of the timing jitter variation and the output pulse shape degradation favours working at higher values of N .

Conclusions

We have provided global design charts for SPM-based 2R regenerators based on normalised regenerator design parameters. We have shown the parameter space for which the TF is optimised, and discussed the compromises between energy efficiency and signal extinction ratio as one moves within this space. In due course it should be possible to extend the analysis to include additional system performance parameters such as resilience to input pulse width variation, shape or chirp [6], and the output timing jitter of the system. The impact of potential inter-pulse effects and stimulated Raman scattering will also ultimately need to be considered and can readily be included in our model.

This work was supported in part by EU FP6 STREP project TRIUMPH.

References

- 1 Mamyshev PV, Proc. ECOC (1998), 475-476.
- 2 Liu X et al., Proc. CLEO (2002), CThAA5, 612-613.
- 3 Her T-H et al., IEEE PTL, Vol.16 (2004), 200-202.
- 4 Taccheo et al., Proc. OFC (2000), ThA1.
- 5 Agrawal GP, Nonlinear fibre optics, Academic press, 3rd ed. (2001).
- 6 Mok JT et al., Opt. Expr., 12, (2004), 4411-4422.